Energy-sharing (*e*,2*e*) collisions: Ionization of the inert gases in the perpendicular plane

F. K. Miller
Physics Department, Old Dominion University, Norfolk, Virginia 23529, USA

H. R. J. Walters
Department of Applied Mathematics and Theoretical Physics, The Queen's University, Belfast, BT7 1NN, United Kingdom

Colm T. Whelan
Physics Department, Old Dominion University, Norfolk, Virginia 23529, USA

(Received 28 May 2014; revised manuscript received 17 October 2014; published 12 January 2015)

The triple differential cross section for ionization of the inert gases He, Ne, Ar, Kr, and Xe in energy-sharing perpendicular plane geometry is investigated. Encouraging agreement with recent experiments is found using the distorted-wave Born approximation (DWBA). Mechanisms are discussed which explain the He and Ne data but which seem to be masked by the greater distortion effects in the heavier targets. The inclusion of postcollisional interaction is explored using Gamow, N_{ee}, and Ward-Macek, M_{ee}, factors. While both help to improve the shape of the cross section for He and Ne at the lower energies, they are not successful for the other targets, and both factors prove to be too strong for all the inert gases with increasing impact energy. It is well known that N_{ee} destroys normalization. Comparing DWBA + M_{ee} results with some absolute experimental points at 1 and 2 eV indicates that it is also not to be trusted on normalization. An interesting situation with Ar is highlighted near 25 eV, where the cross section may be tending towards a strong interference minimum or zero.

DOI: 10.1103/PhysRevA.91.012706 PACS number(s): 34.80.Dp, 34.10.+x

I. INTRODUCTION

An (*e*,2*e*) process is one in which an electron of well-defined energy and momentum is fired at a target and ionizes it and the two exiting electrons are detected in coincidence. The energies and positions in space of these electrons are determined by the experiment, so in effect all but the spin quantum numbers are then known. We can therefore describe it as a kinematically complete experiment; if we could also measure all the spins, we would have all the information from a scattering experiment that quantum mechanics will allow. The technique offers both the possibility of a direct determination of the target wave function and profound insights into the nature of few-body interactions. What information is extracted from such an experiment really depends on the kinematics chosen and the target used. Integrated cross sections can be crude things, and the full power of a highly differential measurement is needed to tease out the intricacies of the interactions. Indeed, often, the most intriguing effects turn up in peculiar geometries where the cross sections are small and where a number of relatively subtle few-body interactions are present. In this paper we are concerned with understanding the low-energy triple differential cross section (TDCS) for electron impact on the inert gases He, Ne, Ar, Kr, and Xe in perpendicular plane geometry. For this study we employ the distorted-wave Born approximation (DWBA). This has proved to be an extremely useful tool for teasing out the different mechanisms and competing effects observed in (*e*,2*e*) processes. For recent reviews, see [1,2]. We use the DWBA here to help understand the shape of the cross sections observed in the recent experiments of [3]. Atomic units ($\hbar = e = m_e = 1$) are used throughout.

II. THE DISTORTED-WAVE BORN APPROXIMATION

The DWBA has been applied to electron impact ionization for quite some time, with the first detailed account being given by [4]; the version we use is, in essential features, the same with some refinements. For a full discussion of the approximation, its strengths, weaknesses, and our computational implementation see [5].

For the ionization of the n,l orbital of an inert gas atom the TCDS, after summing over all final and averaging over all initial spin states, is given by

$$\frac{d^3\sigma^{DWBA}}{d\Omega_f d\Omega_s dE} = 2(2\pi)^4 \frac{k_f k_s}{k_0} \sum_{m=-l}^{l} [|f_{nlm}|^2 + |g_{nlm}|^2 - \mathrm{Re}(f^*_{nlm} g_{nlm})], \quad (1)$$

where

$$\begin{aligned} f_{nlm}(\mathbf{k}_f,\mathbf{k}_s) &= \langle \chi^-(\mathbf{k}_f,\mathbf{r}_f)\chi^-(\mathbf{k}_s,\mathbf{r}_s) \left| \frac{1}{\|\mathbf{r}_f - \mathbf{r}_s\|} \right| \\ &\quad \times \chi_0^+(\mathbf{k}_0,\mathbf{r}_f)\psi_{nlm}(\mathbf{r}_s)\rangle, \\ g_{nlm}(\mathbf{k}_f,\mathbf{k}_s) &= \langle \chi^-(\mathbf{k}_f,\mathbf{r}_s)\chi^-(\mathbf{k}_s,\mathbf{r}_f) \left| \frac{1}{\|\mathbf{r}_f - \mathbf{r}_s\|} \right| \\ &\quad \times \chi_0^+(\mathbf{k}_0,\mathbf{r}_f)\psi_{nlm}(\mathbf{r}_s)\rangle. \end{aligned} \quad (2)$$

Here, χ_0^+ is the distorted wave calculated in the static-exchange potentials of the atom, and χ^- are the distorted waves which are calculated in the static-exchange potentials of the ion and then orthogonalized to ψ_{nlm}. These are normalized to a δ

function, i.e.,

$$\langle \chi^{\pm}(\mathbf{k},\mathbf{r})|\chi^{\pm}(\mathbf{k}',\mathbf{r})\rangle = \delta(\mathbf{k}-\mathbf{k}').$$

In actual calculations, it is not usual to work with the full nonlocal exchange potential; rather, one employs a localized version [5–9]. Its use greatly simplifies the static exchange calculations in that one needs to solve only differential equations rather than the integro-differential equations. Because we treat each of the exiting electrons as moving in the field of a spin-$\frac{1}{2}$ ion, there is an inherent ambiguity in the choice of exchange potential in the final channels; we could chose it to be singlet or triplet [5,10]. For most energies there is little or no difference between results calculated with the singlet and triplet potentials [5,8], but at low energies there is a weakness in the singlet form because for some energies it can become complex. A method has been proposed in [7] to make the potential real again if this happens, but this method results in a discontinuous singlet potential and generally gives results in poorer agreement with experiment than the equivalent triplet calculation (see [5]). In the results presented below we have used the singlet potential for consistency with our earlier calculations [11] except for the lowest energies on helium (see Fig. 3), where the singlet potential breaks down and we use the triplet potential. The DWBA includes the possibility of the incoming electron being elastically scattered in the field of the atom and the exiting electrons being elastically scattered in the field of the ion. The electron-electron interaction occurs exactly once, and no account is taken of postcollisional interactions (pci) between the two final-state electrons or polarization of the target by the incident projectile. For low-energy collisions pci could be important; to take some account of it a Gamow factor N_{ee} [12,13] is sometimes employed,

$$\frac{d^3\sigma^{PCI}}{d\Omega_f d\Omega_s dE} = N_{ee}\frac{d^3\sigma^{DWBA}}{d\Omega_f d\Omega_s dE},$$

where

$$N_{ee} = \frac{\gamma}{e^{\gamma}-1}, \tag{3}$$

with

$$\gamma = \frac{2\pi}{\|\mathbf{k}_f - \mathbf{k}_s\|}.$$

The N_{ee} factor tends to give the dominant angular behavior of the TDCS at low energies due to final-state electron-electron interaction, and it does correctly force the cross section to go to zero when $\mathbf{k}_f = \mathbf{k}_s$. However, the overall normalization is lost. To ameliorate this it is usual to have N_{ee} normalized so that it is fixed to 1 when the angle $\Theta_{fs} = 2\eta$ between $\mathbf{k}_f$ and $\mathbf{k}_s$ is 180°. A modified version of the N_{ee} factor has been suggested by Ward and Macek [14]. These authors suggested replacing N_{ee} with

$$M_{ee} = N_{ee}|{}_1F_1(-i\nu_3, 1, -2ik_3 r_{3av})|, \tag{4}$$

where

$$k_3 = \frac{1}{2}\|\mathbf{k_f} - \mathbf{k_s}\|, \quad \nu_3 = -\frac{1}{\|\mathbf{k_f} - \mathbf{k_s}\|},$$
$$r_{3av} = \frac{3}{\epsilon}\left[\frac{\pi}{4\sqrt{(3)}}\left(1 + \frac{0.627}{\pi}\sqrt{\epsilon}\ln\epsilon\right)\right]^2, \tag{5}$$

with ϵ being the total energy of the two emerging electrons. The factor r_{3av} has been chosen because of the requirement that the M_{ee} factor reproduce the correct Wannier threshold law, and thus it is hoped that the use of M_{ee} rather than N_{ee} will lead to a correctly normalized cross section. Al-Hagan *et al.* [15] recently found that using the M_{ee} factor was helpful in describing the low-energy ionization of molecular hydrogen. Using N_{ee}, or, indeed, M_{ee} for that matter, is a relatively crude way of including pci effects, and it is only really useful very close to the threshold [5].

Despite its inherent simplicity the DWBA has the great advantage that we can explore the relative importance of different effects by "switching" interactions on and off; for example, by replacing $\chi_0^+(\mathbf{k}_0,\mathbf{r}_f)$ in (2) with the plane wave $(2\pi)^{-3/2}\exp(i\mathbf{k}_0\cdot\mathbf{r}_f)$ we switch off the elastic collision between the incident electron and the atom.

III. IONIZATION INTO THE PERPENDICULAR PLANE

For the inert gases there are experimental data for ionization into the perpendicular plane [3]. In these experiments both final-state electrons are detected in the plane perpendicular to the incident electron, $\Phi = 90°$ in Fig. 1 with equal energies $k_f = k_s = k$ and with equal angles $\theta_s = \theta_f = \eta$. The recoil momentum is

$$\mathbf{k_{recoil}} = \mathbf{k_0} - \mathbf{k_f} - \mathbf{k_s}$$
$$\Rightarrow k^2_{recoil} = k_0^2 + 2k^2 + 2k^2\cos\Theta_{fs}. \tag{6}$$

The new experiments [3] are an extension of those of Woolf [16], who presented experimental results for the ionization of helium into the perpendicular plane. Good agreement was found between the earlier results and the DWBA calculations of [11,17]. It should be noted that Θ_{fs} is quoted to be in the range 0° to 360°; of course, the ranges 0° to 180° and 360° to 180° correspond physically to the same process, so the TDCS should be symmetric about $\Theta_{fs} = 180°$. For experiment this is a test of consistency, e.g., alignment of apparatus; for theory it should follow automatically. For ease of comparison with coplanar symmetric [18] and coplanar constant Θ_{fs} [19] geometries we give all our results as a function of the angle $\eta = \frac{\Theta_{fs}}{2}$, so this symmetry will be about 90°.

To understand ionization into the perpendicular plane we must ask how the final-state electrons get into the plane.

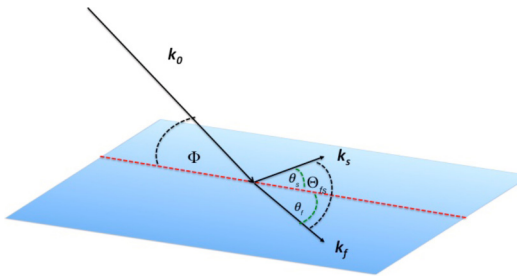

FIG. 1. (Color online) The general experimental setup envisaged for the $(e,2e)$ processes considered in the paper. $\mathbf{k_0},\mathbf{k_f},\mathbf{k_s}$ denote, respectively, the wave vectors of the incident and final-state electrons. $\mathbf{k_0}$ makes an angle Φ with the plane of $\mathbf{k_f}$ and $\mathbf{k_s}$. The exiting electrons are detected with angles θ_f,θ_s left and right of the line defined by $\Phi = 0°$. Their angle of mutual separation is given by $\Theta_{fs} = \theta_f + \theta_s$.

A. Single-scattering mechanism

In a free collision between two electrons with two equal-energy final-state particles conservation of energy and momentum would require that $\mathbf{k_0}, \mathbf{k_f}, \mathbf{k_s}$ all be coplanar and the angle between $\mathbf{k_f}$ and $\mathbf{k_s}$ be 90°. Therefore there can be no ionization into the perpendicular plane for a collision with a free electron. Our target electron is not free, however, but has an initial momentum distribution appropriate to its orbital in the atom. There could be ionization into the perpendicular plane as a result of a collision with an electron of the distribution whose momentum $\boldsymbol{\kappa}$ would exactly cancel out the momentum of the incident electron in the $\mathbf{k}_0$ direction, i.e.,

$$\boldsymbol{\kappa} = -\mathbf{k_0} + \mathbf{k}^{\perp},$$

where $\mathbf{k}^{\perp}$ is perpendicular to $\mathbf{k_0}$. Since

$$\mathbf{k_f} + \mathbf{k_s} = \mathbf{k}^{\perp},$$

the direction of the two outgoing electrons will depend on $\mathbf{k}^{\perp}$.

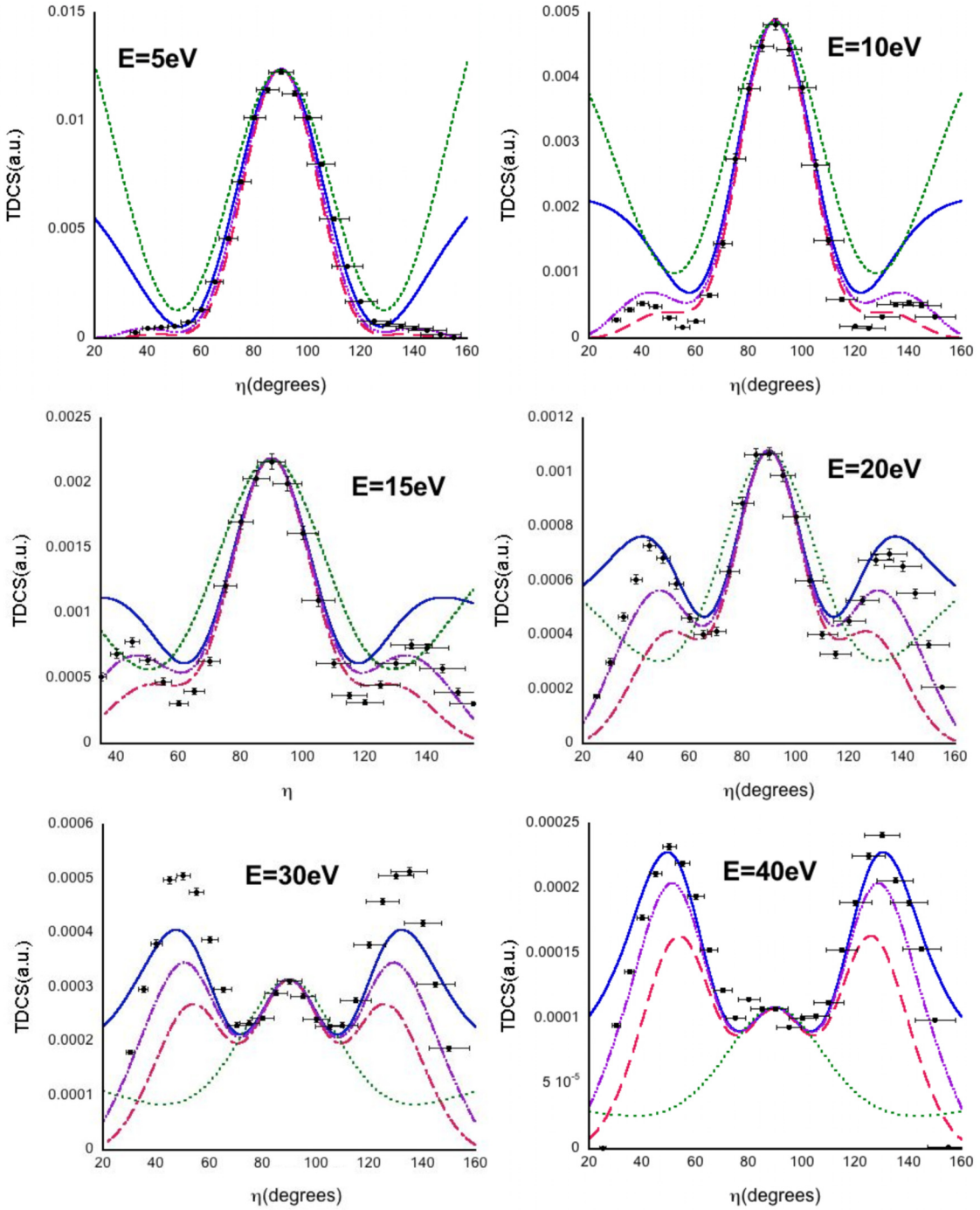

FIG. 2. (Color online) TDCS for perpendicular plane ionization of He(1s) for $E_s = E_f = E$ plotted as a function of the angle $\eta = \frac{\Theta_{fs}}{2}$. Energies E are as shown in each panel; experimental points are from [3]. DWBA: blue solid line; DWBA $+N_{ee}$: red dashed line; DWBA $+ M_{ee}$: purple dash-dotted line; PWA: green dotted line. Experiment is relative and has been normalized to the DWBA at $\eta = 90°$.

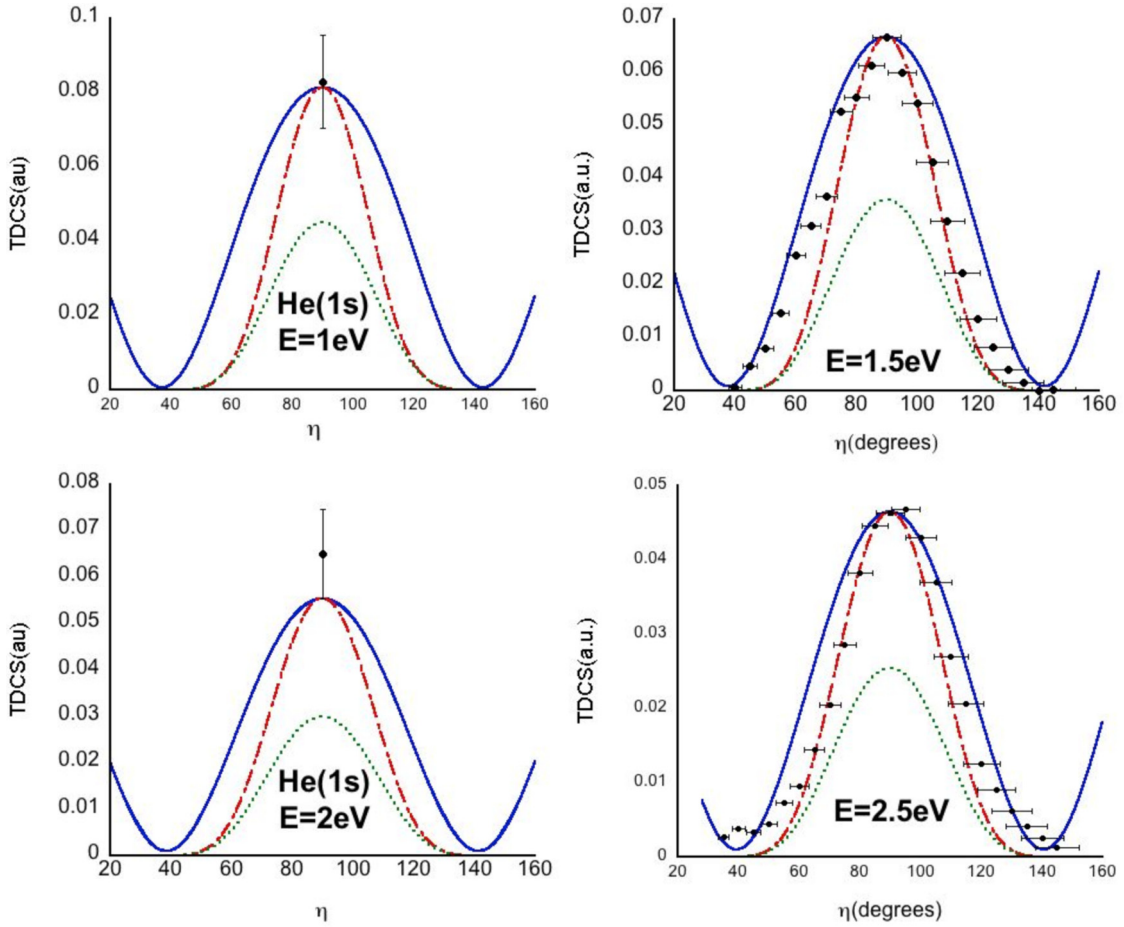

FIG. 3. (Color online) TDCS for perpendicular plane ionization of He(1s) for $E_s = E_f = E$ plotted as a function of the angle $\eta = \frac{\Theta_{fs}}{2}$. Energies E are as shown on each panel. The experimental points are from [3] for $E = 1.5$ and 2.5 eV, are relative, and have been normalized to DWBA. The single experimental points at $E = 1$ and $E = 2$ eV are from [21] and are absolute. DWBA: blue solid line; DWBA $+ N_{ee}$: red dashed line; DWBA $+ M_{ee}$: green dotted line. Note the triplet exchange potential is used in these calculations.

B. Double-scattering mechanism

A second path into the perpendicular plane is the following: the incident electron could be scattered into the perpendicular plane as a result of an elastic collision with the target atom. Then in a second momentum- and energy-conserving free collision the atomic electron is ionized, with both electrons emerging in the perpendicular plane. We have performed calculations for He(1s), Ne(2p), Ar(3p), Kr(4p), and Xe(5p) [20] in (i) the regular DWBA which contains both the single- and double-scattering mechanisms and their interference and very little else, (ii) a model calculation where $\chi_0^+(\mathbf{k}_0, \mathbf{r}_f)$ in (2) is replaced by the incident plane wave $(2\pi)^{-3/2} \exp(i\mathbf{k}_0 \cdot \mathbf{r}_f)$ so that we switch off the elastic collision between the incident electron and the atom [the plane-wave approximation (PWA) then contains only the single-scattering mechanism], and (iii) calculations using both the M_{ee} and the N_{ee} terms to try to get some idea of the importance of pci between the exiting electrons. Since the experiments are relative, we have chosen to normalize the experiment to the DWBA value at $\eta = 90^\circ$. The other approximations are normalized to the same point.

C. Helium(1s)

In Fig. 2 we show a comparison between our calculations and the relative experimental data of [3]. The experiments have been normalized to the DWBA at $\eta = 90^\circ$. The DWBA performs reasonably well at all energies, with the single-scattering maximum at $\eta = 90^\circ$ dominating at low impact energies, while at the higher energies the double-scattering maxima near 45° and 135° become dominant. We also show our plane-wave calculations, which do not contain the double-scattering mechanism and which exhibit only a single-scattering peak at $\eta = 90^\circ$. A feature missing from the straight DWBA is pci. This has the effect of reducing the cross section at small (large) η and will make it zero at $\eta = 0^\circ$ (180°). In order to take pci into account we have repeated our calculations with the N_{ee} and M_{ee} factors, which, in Fig. 2, have each been normalized to unity at $\eta = 90^\circ$. The pci corrected approximations give a reasonable fit to the experimental data at the lower energies, in particular killing the "wings" on the DWBA results at small and large η. The M_{ee} calculations give marginally better shape agreement than N_{ee}.

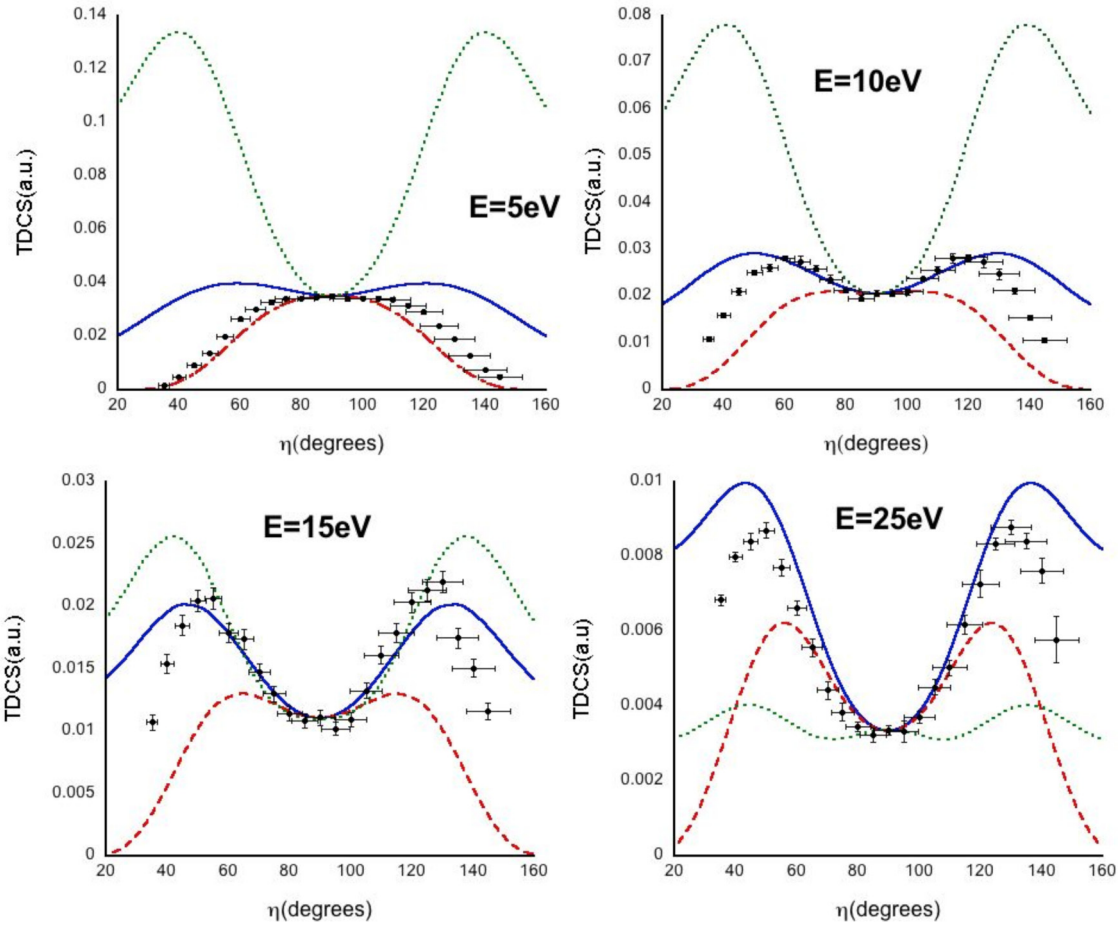

FIG. 4. (Color online) TDCS for the perpendicular plane ionization of Ne($2p$) for $E_s = E_f = E$ plotted as a function of angle $\eta = \frac{\Theta_{fs}}{2}$. Energies E are as shown on each panel; experimental points are from [3]. DWBA: blue solid line; DWBA + N_{ee}: red dashed line; PWA: green dotted line. Experiment is relative and has been normalized to the DWBA at $\eta = 90^\circ$.

It is well known that N_{ee} gives poor results for normalization, producing cross sections that can be much too small. M_{ee} was introduced to correct for this normalization discrepancy. So the question of absolute size is very significant. In addition to the experimental data shown in Fig. 2, Nixon *et al.* [3] also performed measurements at $E = 1.5$ and 2.5 eV. Unfortunately, not exactly at, but near, $E = 1.5$ and 2.5 eV (at $E = 1$ and 2 eV), there are absolute measurements from Rösel and collaborators [21] in the coplanar symmetric geometry. This geometry has one point in common with perpendicular plane geometry, namely, $\eta = 90^\circ$. In Fig. 3 we compare the DWBA, DWBA + absolute M_{ee}, and DWBA + N_{ee} normalized to unity at $\eta = 90^\circ$, with the absolute points from [21] and the relative data from [3] at the these energies. The DWBA agrees well with the absolute points, but the M_{ee}-corrected DWBA clearly fails on normalization. At the nearby energies of $E = 1.5$ and 2.5 eV the DWBA + normalized N_{ee} has good agreement with the relative measurements [3] and, judging by the absolute results at 1 and 2 eV, presumably gives a good representation of the size of these measurements. Since M_{ee} has poor agreement for absolute size and there is only a very small difference in shape compared with that of the N_{ee} calculations, we will not show the M_{ee} results for the other inert gases, with the exception of results for xenon when they are relevant to the comparison with the relativistic calculations of [22].

Finally, we note the calculations of [23] at the two energies $E = 10$ and 20 eV. Those authors also performed DWBA + N_{ee} calculations but added a polarization potential in the initial and final channels. Their results are strikingly different from both our calculations and experiment. The multiple-peak structure seen in Fig. 2 is absent in their results, and they found only a single broad peak centered at $\eta = 90^\circ$.

D. Neon($2p$)

Our results for Ne($2p$) are shown in Fig. 4. In contrast to He($1s$), there is a minimum in the PWA and DWBA cross sections at all energies. The PWA and DWBA both show the development of peaks in the wings. Since the PWA only contains the single-scattering mechanism, these peaks can no longer, in general, be unambiguously attributed solely to the double-scattering mechanism. In PWA they are the result of the interplay of the p-state target orbital and the waves χ^- describing the ejected electrons. However, by $E = 25$ eV the side peaks in PWA have declined significantly, while the DWBA peaks have grown; this is the double-scattering mechanism showing through.

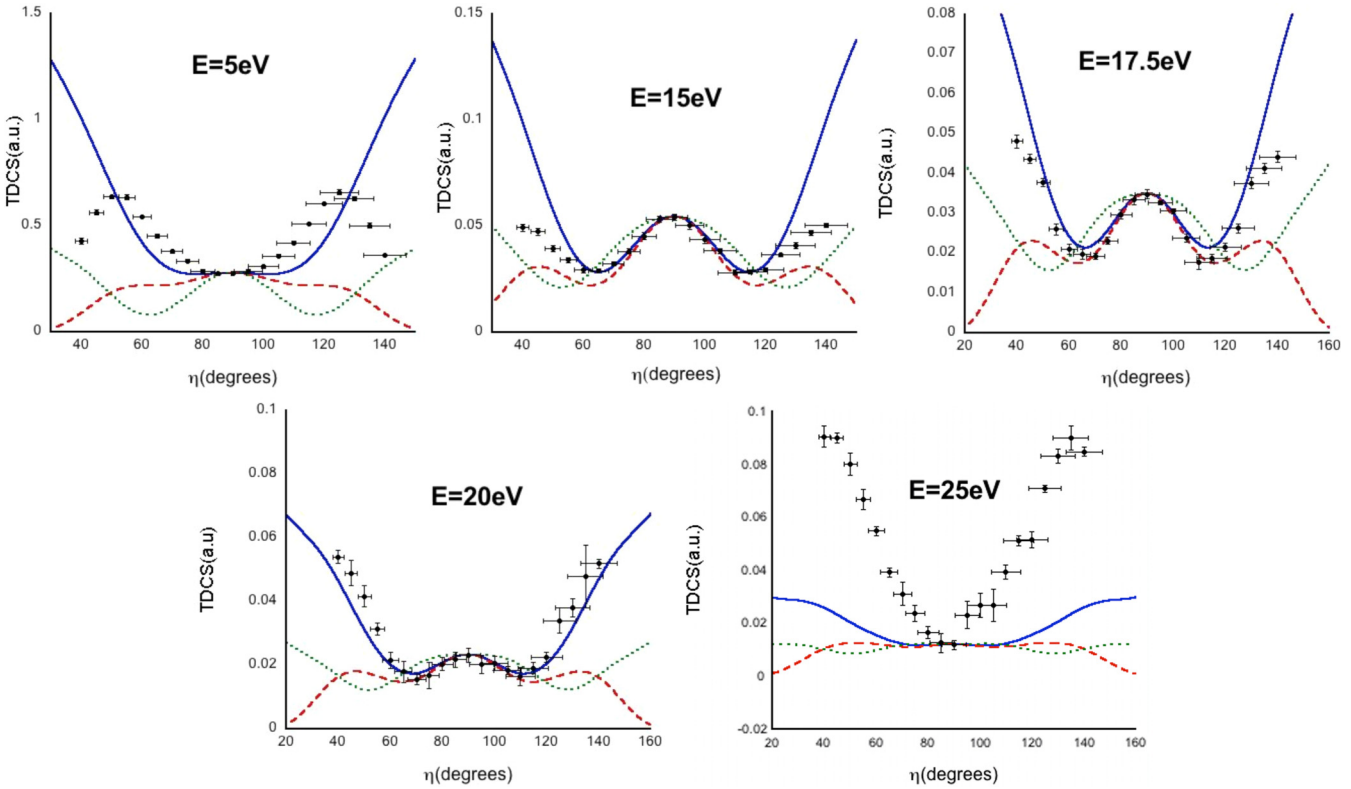

FIG. 5. (Color online) TDCS for perpendicular plane ionization of Ar($3p$) for $E_s = E_f = E$ plotted as a function of angle $\eta = \frac{\Theta_{fs}}{2}$. Energies E are as shown on each panel; experimental points are from [3]. DWBA: blue solid line; DWBA + N_{ee}: red dashed line; PWA: green dotted line. Experiment is relative and has been normalized to the DWBA at $\eta = 90^\circ$.

At 5 eV, it is only when we include pci, through the N_{ee} factor, that we get agreement with experiment. The effect of the pci is to smooth out the minimum in the DWBA at $\eta = 90^\circ$ and turn it into a maximum. While the N_{ee} correction is very helpful at 5 eV, it appears to be too strong at the higher energies where the "pure" DWBA does much better. This is consistent with what we have seen for He($1s$). In Purohit *et al.* [23] results are presented for Ne($2p$) but only at 10 eV and then in their variation of the DWBA, which includes a polarization potential. Their results have the same general form as our DWBA calculations.

E. Argon($3p$)

We show the results for Ar($3p$) in Fig. 5. Here the maximum at $\eta = 90^\circ$ has returned, in both the PW and DWBA approximations, albeit very weakly in DWBA at 5 and 25 eV. In the energy range shown the DWBA does not develop maxima in the wings as we have seen for He($1s$) and Ne($2p$). However, the rapidly rising wings do lead to good agreement with the experimental data at 17.5 and 20 eV. The agreement of DWBA with experiment at 15 eV is also not too bad. For Ar($3p$) the double-scattering mechanism appears to have been buried by other distortion effects.

At 5 eV experiment does show maxima near $\eta = 50^\circ$ and 130°, and one might think that the inclusion of pci, in the form of DWBA + N_{ee}, could bring agreement with experiment as it did for He($1s$) and Ne($2p$). But it does not. Indeed, DWBA + N_{ee} is rather poor for Ar($3p$), except possibly near 15 eV. As with He($1s$) and Ne($2p$), the N_{ee} factor seems to be too strong with increasing energy, much too strong in the case of Ar($3p$). The experimental results at 25 eV, which, like all the other cases in Fig. 5, have been normalized to the DWBA at 90°, seem rather anomalous. Here the shape of the experimental data has changed significantly, adopting a parabolic form with much more pronounced wings. By contrast, the wings on the DWBA appear to be collapsing. This discrepancy between theory and experiment is odd since

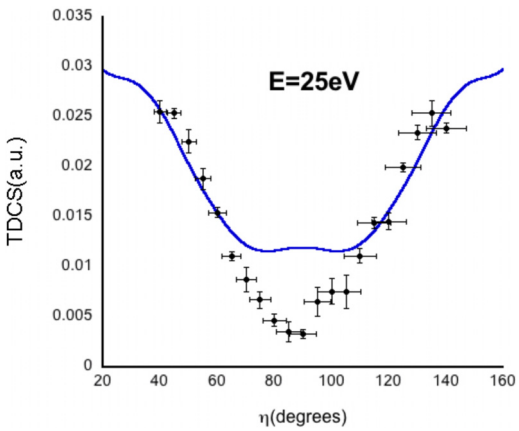

FIG. 6. (Color online) TDCS for perpendicular plane ionization of Ar($3p$) for $E_s = E_f = E = 25$ eV plotted as a function of angle $\eta = \frac{\Theta_{fs}}{2}$. The DWBA calculation as in Fig. 5 and the experimental results of [3], which have now been normalized to the DWBA at 60°, are shown.

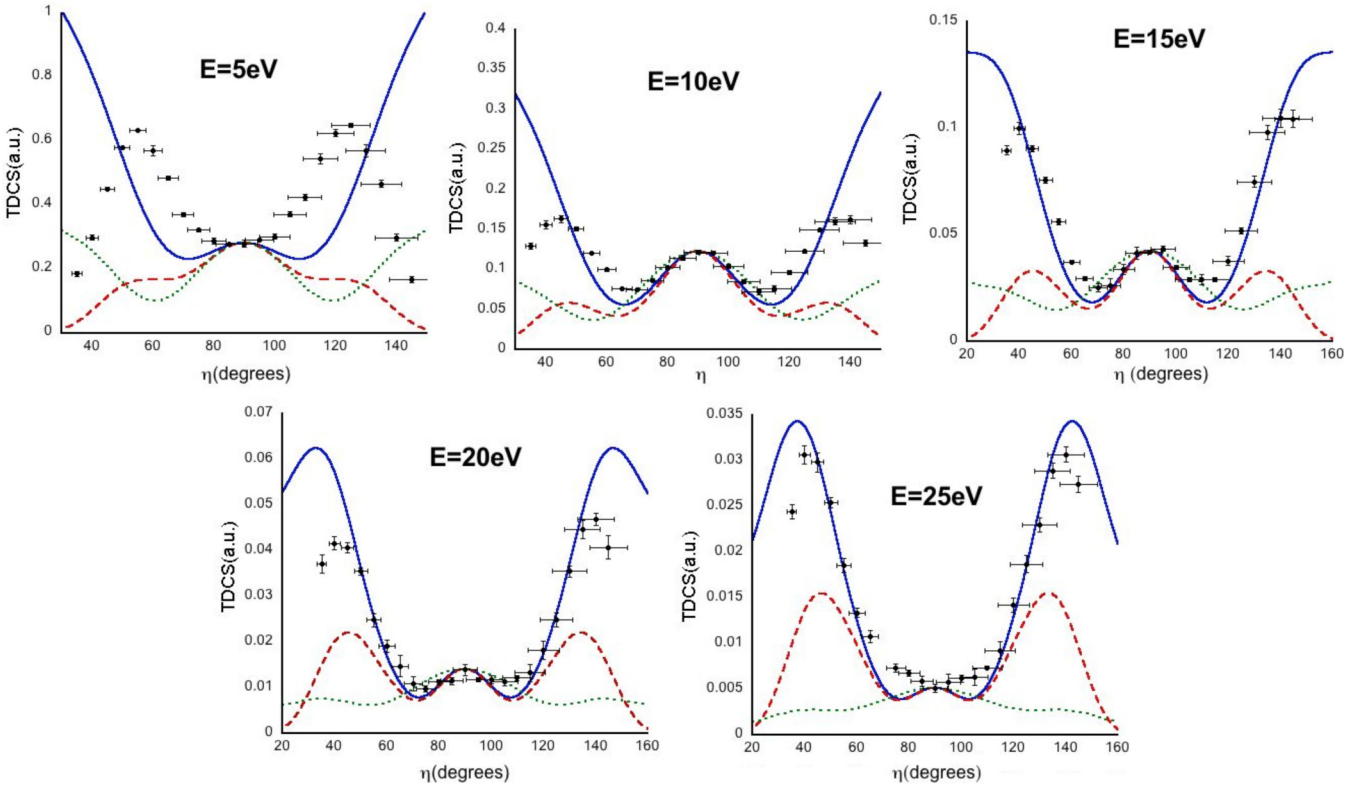

FIG. 7. (Color online) TDCS for perpendicular plane ionization of Kr($4p$) for $E_s = E_f = E$ plotted as a function of the angle $\eta = \frac{\Theta_{fs}}{2}$. Energies E are as shown on each panel; experimental points are from [3]. DWBA: blue solid line; DWBA + N_{ee}: red dashed line; PWA: green dotted line. Experiment is relative and has been normalized to the DWBA at $\eta = 90^\circ$.

for the rest of the inert gases (see Figs. 2, 4, 7, and 8) we get relatively good shape agreement between the experiment of [3] and the DWBA in the region of 25 eV. In Fig. 6 we show the DWBA results for 25 eV once more, but now we have normalized the experiment to the DWBA at 60°. Now there is good agreement in the wings but at the expense of the experimental points reaching a much lower minimum at $\eta = 90^\circ$. This is suggestive of a strong interference effect coming into play, maybe leading to a zero, or near zero, in the cross section. Such an effect was predicted for Li($2s$), Ar($2s$), and Ne($2s$) in [24] and was subsequently observed in neon experiments [25]. Rasch *et al.* [24] also examined Ar($2p$) and Ne($2p$) but found that the effect could be masked by the different behaviors of the magnetic sublevels. The observation of interference effects is very sensitive to the kinematics of the measurements. More detailed experimental investigation in the region between 20 and 30 eV is recommended.

F. Krypton($4p$)

Our results for Kr($4p$) are shown in Fig. 7. Except at 25 eV, the results are not too dissimilar from those for Ar($3p$). In particular, DWBA is in quite good agreement with experiment at 15 eV and above. Unlike Ar($3p$), both DWBA and experiment develop distinct peaks at small and large η. However, PWA also has such peaks, although not as pronounced, so it is difficult to attribute them to the double-scattering mechanism. As with Ar($3p$), DWBA + N_{ee} is poor, and the pci effect, as described by the N_{ee} factor, is too strong. The results at 25 eV contrast strongly with the Ar($3p$) case, both in the shape of the experimental points and in their agreement with DWBA.

G. Xenon($5p$)

For Xe($5p$) (Fig. 8), our plane-wave approximation gives something of the character of the cross section at all energies. At 10 and 15 eV the DWBA gives some structure which is, to some degree, mirrored by the experiment. At higher energies these structures disappear. The M_{ee} and N_{ee} factors only make a relatively small difference to shape. All in all, the DWBA is in reasonable agreement for all energies.

There are fully relativistic DWBA calculations from Illarionov and Stauffer [22] with which to compare the results for Xe($5p$). While both sets of calculations tend to produce the same general trend there are a number of puzzling discrepancies. Naively, one would expect that the nonrelativistic and relativistic calculations would be very similar [26]. In [22] an M_{ee} factor is included, so we include the M_{ee} results in Fig. 8. In [22], at 5 eV, there is a single central peak with only a slight indication of structure in the wings, while our DWBA + M_{ee} shows a central peak and two well-defined, if smaller, peaks in the wings. At 10 eV our calculation and theirs seem to have reasonable agreement, but at 15 eV the large-angle peaks are more pronounced in [22]; indeed, they are bigger than the central peak. The large-angle peaks remain clearly visible in their calculations for all the remaining energies but are essentially eliminated in our DWBA + M_{ee} calculations above 20 eV.

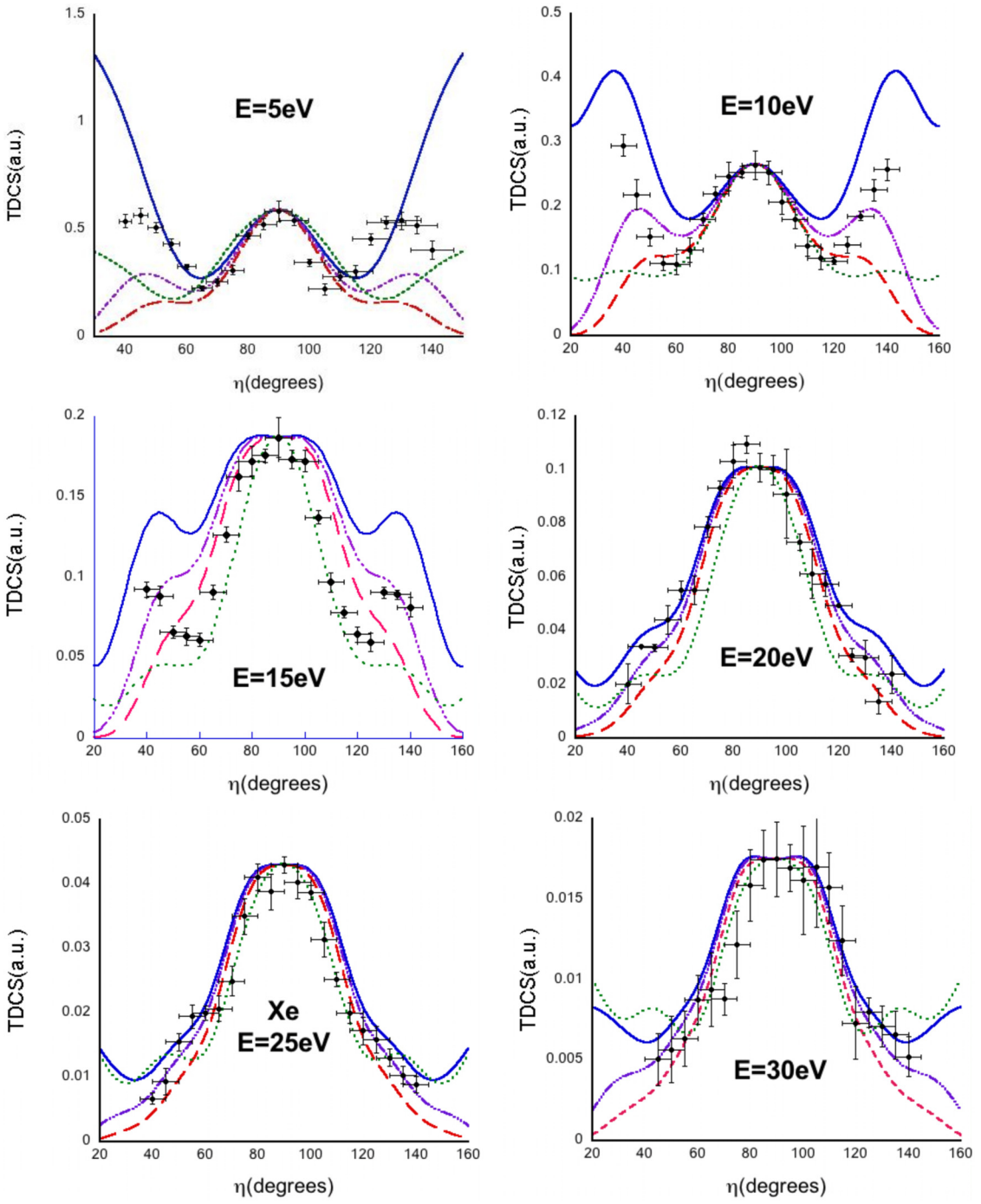

FIG. 8. (Color online) TDCS for perpendicular plane ionization of Xe($5p$),$^2P_{\frac{3}{2}}$, for $E_s = E_f = E$ plotted as a function of the angle $\eta = \frac{\Theta_{fs}}{2}$. Energies E are as shown in each panel; experimental points are from [3]. DWBA: blue solid line; DWBA + N_{ee}: red dashed line; DWBA + M_{ee}: purple dash-dotted line; PWA: green dotted line. Experiment is relative and has been normalized to the DWBA at $\eta = 90^\circ$.

IV. CONCLUSION

We have considered the ionization of the inert gases in the perpendicular plane geometry and have compared our results with the relative experimental measurements of [3]. We have used the DWBA as our basic approximation. This approximation includes the single- and double-scattering mechanisms proposed by Zhang *et al.* [11]. However, except for the lightest gases, He and Ne, we have been unable to identify these mechanisms. That is not to say that they do not exist but rather that the distortion effects are so strong in the heavier gases that they get masked. Agreement between our DWBA calculations and the experiment is very encouraging, especially for He and Xe.

At the lowest energies pci are very important. We have tried to include them by using the Gamow factor N_{ee} and the Ward-Macek factor M_{ee}. For He and Ne these factors are very effective at improving the shape of the low-energy

TDCS, but they fail for the heavier inert gases Ar, Kr, and Xe. Also, with increasing energy the N_{ee} and M_{ee} factors become much too strong, distorting the shape of the DWBA away from the experimental results. Here the straight DWBA is in very much better agreement with experiment. It is also well known that the N_{ee} factor fails dramatically on normalization. To correct for this defect we have normalized it to unity at $\eta = 90^\circ$. We have also used the same renormalization of the M_{ee} factor. However, M_{ee} was introduced to correct for the normalization defect of N_{ee} and should be able to stand on its own without renormalization. We have tested this for He at impact energies of 1 and 2 eV, for which we have absolute points from the coplanar measurements from [21]. We find that here unrenormalized M_{ee} gives cross sections that are too small by a factor of 2, while the "pure" DWBA gives agreement. Clearly, M_{ee}, although giving a much better representation of normalization than N_{ee}, is not to be trusted on normalization. A better approach for including pci is needed

Ar presents an interesting case. Like all the other inert gases, agreement between the experiment of [3] and DWBA generally improves above 15 eV impact energy, except that there is a sudden discrepancy at 25 eV. Here normalization of the experiment to DWBA at $\eta = 90^\circ$ would seem to imply that there is something seriously wrong either with experiment or theory. But normalization at $\eta = 60^\circ$ is suggestive of an approaching zero, or near zero, in the TDCS as a result of strong interference effects, with theory and experiment not quite agreeing on how rapidly the approach occurs for such a delicate effect. This needs to be examined more carefully both experimentally and theoretically.

[1] D. H. Madison and O. Al-Hagan, J. At. Mol. Opt. Phys. **2010**, 367180 (2010).

[2] C. T. Whelan, in *Fragmentation Processes: Topics in Atomic and Molecular Physics*, edited by Colm T. Whelan (Cambridge University Press, Cambridge, 2013), p. 207.

[3] K. L. Nixon, A. J. Murray, and C. Kaiser, J. Phys. B **43**, 085202 (2010).

[4] D. H. Madison, R. V. Calhoun, and W. N. Shelton, Phys. Rev. A **16**, 552 (1977).

[5] J. Rasch, Ph.D. thesis, University of Cambridge, 1996.

[6] J. B. Furness and I. E. Mc Carthy, J. Phys. B **6**, 2280 (1973).

[7] M. E. Riley and D. G. Truhlar, J. Chem. Phys. **63**, 2182 (1975).

[8] B. H. Bransden, M. R. C. McDowell, C. J. Noble, and T. Scott, J. Phys. B **9**, 1301 (1976).

[9] J. M. Martinez, H. R. J. Walters, and C. T. Whelan, J. Phys. B **41**, 065202 (2008).

[10] E. P. Curran and H. R. J. Walters, J. Phys. B: At. Mol. Phys. **20**, 337 (1987).

[11] X. Zhang, C. T. Whelan, and H. R. J. Walters, J. Phys. B **23**, L173 (1990).

[12] J. Botero and J. H. Macek, Phys. Rev. Lett. **68**, 576 (1992).

[13] J. Röder, J. Rasch, K. Jung, C. T. Whelan, H. Ehrhardt, R. J. Allan, and H. R. J. Walters, Phys. Rev. A **53**, 225 (1996).

[14] S. J. Ward and J. H. Macek, Phys. Rev. A **49**, 1049 (1994).

[15] O. Al-Hagan, C. Kaiser, D. Madison, and A. J. Murray, Nat. Phys. **5**, 59 (2009).

[16] M. B. J. Woolf, Ph.D. thesis, University of Manchester, 1989.

[17] C. T. Whelan, R. J. Allan, H. R. J. Walters, and X. Zhang, in *(e, 2e) and Related Processes*, edited by Colm T. Whelan, H. R. J. Walters, A. Lahmam-Bennani, and H. Ehrhardt (Kluwer, Dordrecht, 1993), p. 1.

[18] A. Pochat, X. Zhang, C. T. Whelan, H. R. J. Walters, R. J. Tweed, F. Gélébart, M. Cherid, and R. J. Allan, Phys. Rev. A **47**, R3483 (1993).

[19] C. T. Whelan, R. J. Allan, J. Rasch, H. R. J. Walters, X. Zhang, J. Röder, K. Jung, and H. Ehrhardt, Phys. Rev. A **50**, 4394 (1994).

[20] We are using the notation $A(nl)$ to mean the ionization of the n,l electron from atom A. For example, Ne$(2p)$ represents the processes:

$$e^- + \mathrm{Ne}(1s^2,2s^2,2p^6) \rightarrow e^- + e^- + \mathrm{Ne}(1s^2,2s^2,2p^5),$$

while Ar$(3p)$ is the process

$$e^- + \mathrm{Ar}(1s^2,2s^2,2p^6,3s^2,3p^6) \rightarrow e^- + e^- + \mathrm{Ar}(1s^2,2s^2,2p^6,3s^2,3p^5).$$

[21] T. Rösel, J. Röder, L. Frost, K. Jung, H. Ehrhardt, S. Jones, and D. H. Madison, Phys. Rev. A **46**, 2539 (1992); see also H. Ehrhardt and T. Rösel, in *(e, 2e) and Related Processes*, edited by Colm T. Whelan, H. R. J. Walters, A. Lahmam-Bennani, and H. Ehrhardt (Kluwer, Dordrecht, 1993), p. 75.

[22] A. A. Illarionov and A. D. Stauffer, J. Phys. B **45**, 225202 (2012).

[23] G. Purohit, A. S. Bhullar, and K. K. Sud, Indian J. Phys. **77B**, 177 (2003).

[24] J. Rasch, C. T. Whelan, R. J. Allan, S. P. Lucey, and H. R. J. Walters, Phys. Rev. A **56**, 1379 (1997).

[25] A. J. Murray and F. H. Read, Phys. Rev. A **63**, 012714 (2000).

[26] S. Keller, C. T. Whelan, H. Ast, H. R. J. Walters, and R. M. Dreizler, Phys. Rev. A **50**, 3865 (1994).